J. Automation & Systems Engineering 11-3 (2017): 208-221

Regular paper

Speed Control for PMSM Drive System Using Predictive Control

Badre Bossoufi [1]Ahmed Lagrioui[2]

[1]Higher School of Technology, University of Mohammed I, Oujda, Morocco

[2]ENSAM Mekness, Morocco

Abstract-This paper presents a new contribution for the control technique of a permanent magnets synchronous (PMSM) drive, this technique based on newly nonlinear Predictive Control. This control technique is based on the Taylor series expansion. The nonlinear predictive controller minimum variance (CPNLVM) has the objective of minimizing the error between the model output of the system and the output of the reference model. The operating principle of our approach is presented and analyzed at first, later the validation of our model is realized on Matlab & Simulink. The results obtained show the robustness and efficiency of this technique.

Keywords: Predictive Control, Speed Control, Permanent Magnet Synchronous Machine (PMSM), Robust Adaptive Control.

1. INTRODUCTION

The PMSM motor is attractive candidates for high performance applications such as machine tools, or direct drive robotics. The effects of torque ripple on PMSM drives in such applications are potentially significant, as the high-frequency dynamics of the actuated system may get excited.

The PMSMs motors are known to provide higher torque per unit volume and better efficiency than induction motors, while improvements in the properties of permanent-magnet materials have increased their viability. Recently, sensorless PMSM drives have received increasing interest for industrial applications where there are limitations on the use of a position sensor. The elimination of the position sensor reduces the cost of the drive and increases the overall system ruggedness and reliability. High performance operation of sensorless PMSM drives mainly relies on accurate knowledge of the rotor-magnet flux magnitude, position, and speed. The sensorless rotor-position estimation techniques can be classified into two major groups: the motor model-based and the rotor-saliency-based techniques. The latter are suitable only for the interior PMSM (IPMSM). Most of the motor-model-based techniques detect the back-EMF vector, which holds information about the rotor position and speed, using either open-loop estimators [3] or closed-loop estimators/observers. In other motor-model-based techniques, the rotor-flux vector is directly estimated [2]. Moreover, adaptive observers have been used to estimate the stator current, the rotor speed, and the rotor position [1].

The nonlinear predictive controller a minimum variance (CPNLVM) is based on the Taylor series expansion; it has the objective of minimizing the error between the model output of the system and the output of the reference model.

The major disadvantage of this controller lies in the lack of the screw to robustness to modeling errors, and the variation of the load torque. To overcome this disadvantage, model error and the change in load torque will be taken into account in the model of the machine and will be assumed to be unknown and immeasurable disturbance but bounded in time. It is therefore necessary to estimate. To this end, we have proposed a disturbance estimator based on a new design function l(x), since the relative degree of the disturbance (load torque) affecting the regulation of the speed is lower than the control. In addition, we have designed an anti-saturation diagram, and, from the consideration of limiting blocks of variables manipulated in the design of the estimator [7].

2. NON-LINEAR MODEL OF THE PERMANENT MAGNETS SYNCHRONOUS MACHINE

Taking into account the disturbances affecting the regulation of the output, the model of the synchronous motor with permanent magnets set in a reference frame fixed to the rotor (d, q) is described by [4]:

$$\begin{cases} \dot{x} = f(x) + g_1 u + g_2 b \\ y = h(x) \end{cases} \tag{1}$$

$$u = \begin{bmatrix} u_{sd} \\ u_{sq} \end{bmatrix}; \qquad x = \begin{bmatrix} i_{sd} \\ i_{sq} \\ \Omega \end{bmatrix}; \qquad y = \begin{bmatrix} y_1 \\ y_2 \end{bmatrix} = \begin{bmatrix} i_{sd} \\ \Omega \end{bmatrix}; \qquad b = \begin{bmatrix} f_d \\ f_\Omega \end{bmatrix} \tag{2}$$

$$g_1 = \begin{bmatrix} g_d & g_q \end{bmatrix} = \begin{bmatrix} \frac{1}{L_{sd}} & 0 \\ 0 & \frac{1}{L_{sq}} \\ 0 & 0 \end{bmatrix}; \qquad g_2 = \begin{bmatrix} b_d & b_q \end{bmatrix} = \begin{bmatrix} -\frac{1}{L_{sd}} & 0 \\ 0 & 0 \\ 0 & -\frac{1}{J} \end{bmatrix} \tag{3}$$

With :

$$f(x) = \begin{bmatrix} f_1(x) \\ f_2(x) \\ f_3(x) \end{bmatrix} = \begin{bmatrix} -\frac{R_s}{L_{sd}}.i_{sd} + p\frac{L_{sq}}{L_{sd}}.i_{sq}.\Omega \\ -\frac{R_s}{L_{sq}}.i_{sq} - p\frac{L_{sd}}{L_{sq}}.i_{sd}.\Omega - p\frac{\Phi_f}{L_{sq}}.\Omega \\ -\frac{f}{J}.\Omega + \frac{3p}{2J}(L_{sd} - L_{sq}).i_{sd}.i_{sq} + \frac{3p}{2J}\Phi_f.i_{sq} \end{bmatrix} \tag{4}$$

Where b is the disturbance that affects the regulation of outputs, its dynamics is supposed slow compared to other state variables. We can write:

$$\frac{db}{dt} = 0 \tag{5}$$

3. NON-LINEAR PREDICTIVE CONTROLLER MINIMUM VARIANCE (CPNLVM)

Under the principle of predictive control to minimum variance, the cost function used to develop predictive control law for the synchronous permanent magnet motor is written as follows [5]:

$$\Im = \frac{1}{2}\int_0^{T_1}\left(e_d(t+\tau)\right)^2 d\tau + \frac{1}{2}\int_0^{T_2}\left(e_\Omega(t+\tau)\right)^2 d\tau \tag{6}$$

$$\begin{cases} e_d(t+\tau) = y_{1r}(t+\tau) - y_1(t+\tau) \\ e_\Omega(t+\tau) = y_{2r}(t+\tau) - y_2(t+\tau) \end{cases} \tag{7}$$

Where: τ is the prediction time.

$y_i(t+\tau)$ is the prediction of the output to τ step.

$y_{ir}(t+\tau)$ is the reference path to the future.

It should be noted that for the synchronous machine with permanent magnets, exits the future are given by [6]:

$$\begin{cases} \left[y_1(t+T_1) \quad y_2(t+T_2)\right]^T = \left[i_{sd}(t+T_1) \quad \Omega(t+T_2)\right]^T \\ \left[y_{1r}(t+T_1) \quad y_{2r}(t+T_2)\right]^T = \left[i_{sdref}(t+T_1) \quad \Omega_{ref}(t+T_2)\right]^T \end{cases} \tag{8}$$

The objective of this strategy is to find the controls that minimize the performance criterion defined by (7).

The outputs and their references to the future are calculated approximately by the Taylor series expansion. The differentiation of the output yi and yir reference with respect to time is repeated ρi time to bring up the command, hence [8]:

$$\begin{cases} \left[y_1(t+\tau) \quad y_2(t+\tau)\right]^T = \Gamma(\tau)Y(t) \\ \left[y_{1r}(t+\tau) \quad y_{2r}(t+\tau)\right]^T = \Gamma(\tau)Y_r(t) \end{cases} \tag{9}$$

With

$$\begin{cases} Y(t) = \left[y_1 \quad y_2 \quad \dot{y}_1 \quad \dot{y}_2 \quad \ddot{y}_2\right]^T \\ Y_r(t) = \left[y_{1r} \quad y_{2r} \quad \dot{y}_{1r} \quad \dot{y}_{2r} \quad \ddot{y}_{2r}\right]^T \end{cases} \tag{10}$$

$$\Gamma(\tau) = \begin{bmatrix} \Gamma_1(\tau) \\ \Gamma_2(\tau) \end{bmatrix} = \begin{bmatrix} 1 & 0 & \tau & 0 & 0 \\ 1 & 1 & 0 & \tau & \dfrac{\tau^2}{2} \end{bmatrix} \tag{11}$$

Using (9), the quadratic performance criterion defined by (6) can be simplified as follows:

$$\Im = \frac{1}{2}\left(Y(t) - Y_r(t)\right)^T \Lambda(T_1, T_2)\left(Y(t) - Y_r(t)\right) \tag{12}$$

$$\Lambda(T_1, T_2) = \int_0^{T_1} (\Gamma_1(\tau))^T \Gamma_1(\tau) d\tau + \int_0^{T_2} (\Gamma_2(\tau))^T \Gamma_2(\tau) d\tau \tag{13}$$

In developing the above expression, we get:

$$\Lambda(T_1,T_2)=\begin{bmatrix} T_1 & 0 & \frac{T_1^2}{2} & 0 & 0 \\ 0 & T_2 & 0 & \frac{T_2^2}{2} & \frac{T_2^3}{6} \\ \frac{T_1^2}{2} & 0 & \frac{T_1^3}{3} & 0 & 0 \\ 0 & \frac{T_2^2}{2} & 0 & \frac{T_2^3}{3} & \frac{T_2^4}{8} \\ 0 & \frac{T_2^3}{6} & 0 & \frac{T_2^4}{8} & \frac{T_2^5}{20} \end{bmatrix} \tag{14}$$

Combining (5) and (10) we get:

$$Y(t)-Y_r(t)=\begin{bmatrix} y_1(t)-y_{1r}(t) \\ y_2(t)-y_{2r}(t) \\ L_f h_1(x)-\dot{y}_{1r}(t) \\ L_f h_2(x)-\dot{y}_{2r}(t) \\ L_f^{\,2} h_2(x)-\ddot{y}_{2r}(t) \end{bmatrix}+\begin{bmatrix} 0_{1\times 2} \\ 0_{1\times 2} \\ L_{g_1} h_1(x) \\ 0_{1\times 2} \\ L_{g_1} L_f h_2(x) \end{bmatrix} u(t)+\begin{bmatrix} 0_{1\times 2} \\ 0_{1\times 2} \\ L_{g_2} h_1(x) \\ L_{g_2} h_2(x) \\ L_{g2} L_f h_2(x) \end{bmatrix} b(t) \tag{15}$$

In the absence of stresses, the control law minimizing the cost function is obtained by solving the following equation [9]:

$$\frac{d\Im}{du}=0 \tag{16}$$

This amounts to solving the following system of equations:

$$\frac{d\Im}{du}=\left(\frac{d}{du}(Y(t)-Y_r(t)\right)^T \Lambda(T_1,T_2)\big(Y(t)-Y_r(t)\big)=0 \tag{17}$$

Cela est équivalent à :

$$\left(\begin{bmatrix} 0_{1\times 2} \\ 0_{1\times 2} \\ L_{g_1} h_1(x) \\ 0_{1\times 2} \\ L_{g_1} L_f h_2(x) \end{bmatrix}\right)^T \Lambda(T)\left(\begin{bmatrix} y_1(t)-y_{1r}(t) \\ y_2(t)-y_{2r}(t) \\ L_f h_1(x)-\dot{y}_{1r}(t) \\ L_f h_2(x)-\dot{y}_{2r}(t) \\ L_f^{\,2} h_2(x)-\ddot{y}_{2r}(t) \end{bmatrix}+\begin{bmatrix} 0_{1\times 2} \\ 0_{1\times 2} \\ L_{g_1} h_1(x) \\ 0_{1\times 2} \\ L_{g_1} L_f h_2(x) \end{bmatrix} u(t)+\begin{bmatrix} 0_{1\times 2} \\ 0_{1\times 2} \\ L_{g_2} h_1(x) \\ L_{g_2} h_2(x) \\ L_{g2} L_f h_2(x) \end{bmatrix} b(t)\right)=0 \tag{18}$$

This results in the following optimal solution:

$$u(t)=G_1(x)^{-1}\left(\begin{bmatrix} \sum_{i=0}^{1} K_i^1\left(y_{1r}^{(i)}(t)-L_f^i h_1(x)\right) \\ \sum_{i=0}^{2} K_i^2\left(y_{2r}^{(i)}(t)-L_f^i h_2(x)\right) \end{bmatrix}-G_2(x)b(t)\right) \tag{19}$$

$$\begin{cases} K_0^1=\dfrac{3}{2T_1}; K_1^1=1 \\ K_0^2=\dfrac{10}{3T_2^2}; K_1^2=\dfrac{5}{2T_2}; K_2^2=1 \end{cases} \tag{20}$$

The expression of the matrix G1(x) is the same as that developed for the minimum variance predictive control, and is defined by (6).

In the case of the generalized predictive control matrix G2(x) is given by:

$$G_2(x)=\begin{bmatrix} L_{g_2}h_1(x) \\ L_{g_2}L_f h_2(x)+K_1^2 L_{g_2}h_2(x) \end{bmatrix}=\begin{bmatrix} -\dfrac{1}{L_{sd}} & 0 \\ -\dfrac{3p(L_{sd}-L_{sq})i_{sq}}{2JL_{sd}} & \dfrac{1}{J}\left(-K_1^2+\dfrac{f}{J}\right) \end{bmatrix} \tag{21}$$

Knowing the value of the disturbance, the dynamic error evolves according to the following equation:

$$\begin{cases} K_0^1 e_d(t)+K_1^1 \dot{e}_d(t)=0 \\ K_0^2 e_\Omega(t)+K_1^2 \dot{e}_\Omega(t)+K_2^2 \ddot{e}_\Omega(t)=0 \end{cases} \tag{22}$$

Equation leads to the following roots:

$$\begin{cases} s_{1d}=-\dfrac{3}{2T_1} \\ s_{1\Omega}=-\dfrac{1.25}{T_2}-i\dfrac{1{,}3307}{T_2} \\ s_{2\Omega}=-\dfrac{1.25}{T_2}+i\dfrac{1{,}3307}{T_2} \end{cases} \tag{23}$$

From (23), we deduce that the closed loop system is stable. On the other hand, we note that a small prediction time results in a quick response. This is at the expense of effort control [10].

In cases where the extent of the disruption is not available, it will be replaced by its estimate. In the same manner as for the minimum variance predictive control, the disturbance estimator, in the absence of saturation of blocks, can be written in the following form:

$$\hat{b}(t)=\begin{bmatrix} \mu_d\left(K_0^1\int_0^t e_d(\tau)d\tau+e_d(t)\right) \\ \mu_\Omega\left(K_0^2\int_0^t e_\Omega(\tau)d\tau+K_1^2 e_\Omega(t)+\dot{e}_\Omega(t)\right) \end{bmatrix} \tag{24}$$

We also show that the stability of the observer (24) is provided by:

$$\frac{\mu_d}{L_{sd}}<0 \quad ; \quad \mu_\Omega\left(\frac{K_1^2}{J}-\frac{f}{J^2}\right)<0 \tag{25}$$

In case of saturation of blocks are used to limit the voltage from the controller, the control law takes the following form:

$$u(t)=\begin{bmatrix} u_{dref}(t) \\ u_{qref}(t) \end{bmatrix}=\begin{bmatrix} u_d^*(t) \\ u_q^*(t) \end{bmatrix}+\begin{bmatrix} \overline{u}_d(t) \\ \overline{u}_q(t) \end{bmatrix}=u^*(t)+\overline{u}(t) \tag{26}$$

$$u^*(t)=G_1(x)^{-1}\left(\begin{bmatrix} \sum_{i=0}^{1} K_i^1\left(y_{1r}^{(i)}(t)-L_f^i h_1(x)\right) \\ \sum_{i=0}^{2} K_i^2\left(y_{2r}^{(i)}(t)-L_f^i h_2(x)\right) \end{bmatrix}+G_2(x)\hat{b}^*(t)\right) \tag{27}$$

$$\overline{u}(t)=-\left(G_1(x)^{-1}G_2(x)\mu\int_0^t G_1(x)\big(u(\tau)-sat(u(\tau))\big)d\tau\right) \tag{28}$$

The limit values of the manipulated variables are the same as those developed for predictive control to minimum variance.

4. RESULTS AND SIMULATIONS

The CPNLVM controller parameters are: the controller sampling time Tsc=50μs, the prediction time for the current control T1=0,5ms and the prediction time for the speed control T2=5ms. In addition, to ensure the stability of the observer, we μd=-0.1 and μΩ=0.00001.

To evaluate the performance of the nonlinear predictive controller minimum variance, we performed simulations using the following steps:

- To test the continued trajectory, the speed reference was made variable. The reference direct current component has been set at zero.
- To test the robustness of the controller, the electrical and mechanical parameters are varied in the predictive controller at t = 0.2s. Indeed, the value of the resistance and the inductance quadrature becomes equal to the half of the nominal value (Rs=0.5Rsn, Lsq=0.5Lsqn) while the value of the direct inductance becomes equal to twice its nominal value (Lsd=0.5Lsdn). On the other hand, the value of the magnetic flux is increased by 20% of its nominal value (Φf=1.2Φfn). As regards the mechanical parameters (damping coefficient and moment of inertia), they become equal to half of their nominal values (f=0.5fn, J=0.5Jn).
- In order to test the performance of the Controller at the disturbance rejection, apply a load torque of 2 Nm at t = 0.3s.
- Finally, to test the effectiveness of anti-saturation diagram, the speed set point is passed through a second order filter whose dynamics are chosen very fast so that the phase current exceeds transient, its maximum value. This allows testing the effectiveness of the anti-saturation diagram when the dynamic of the reference speed is too fast.

The control structure for carrying out the direct CPNLVM structure on the permanent magnet synchronous machine is illustrated in the following block diagram:

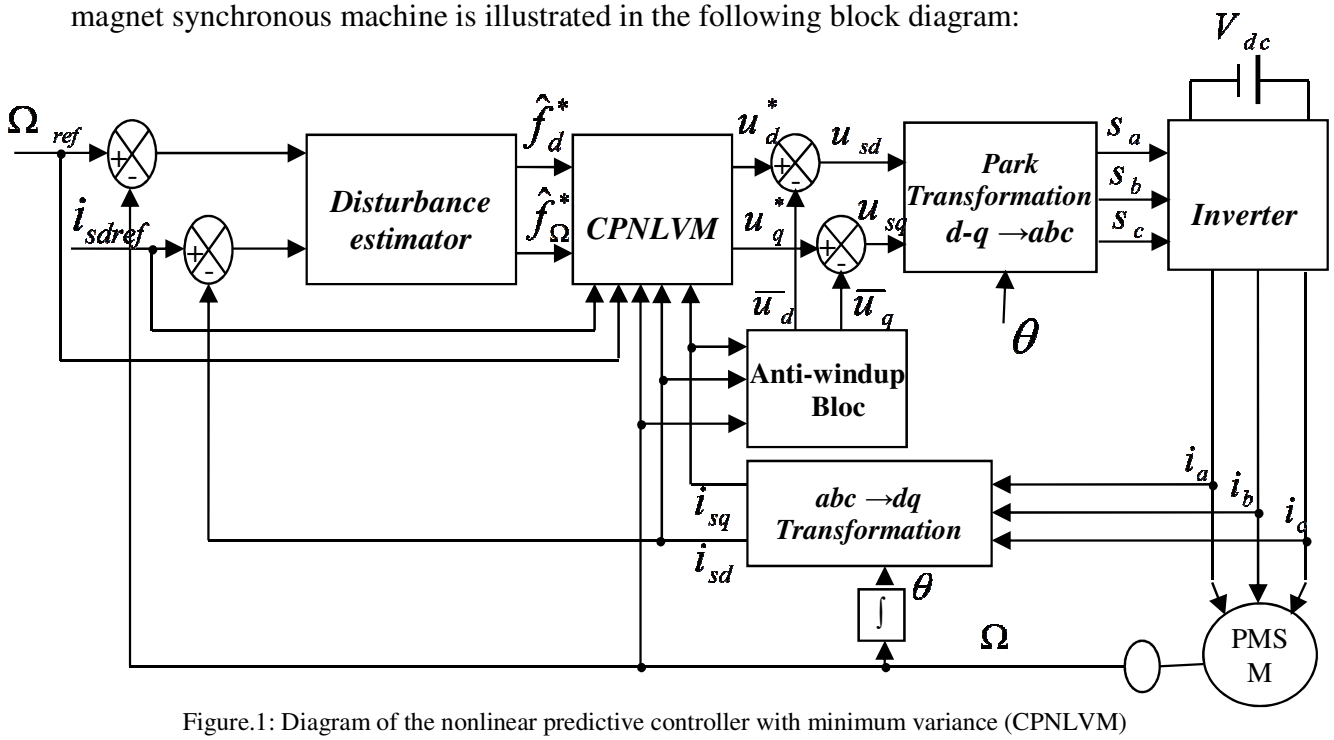

Figure.1: Diagram of the nonlinear predictive controller with minimum variance (CPNLVM)

4.1. Follow of the speed trajectory

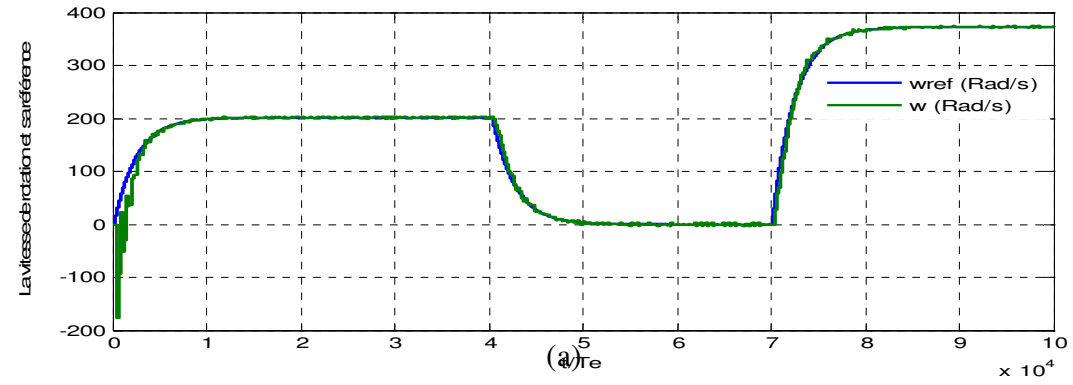

(a)

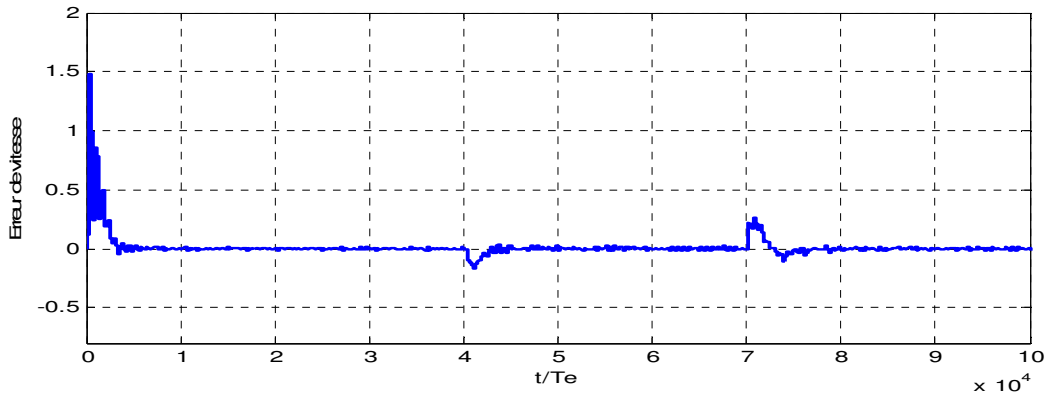

(b)

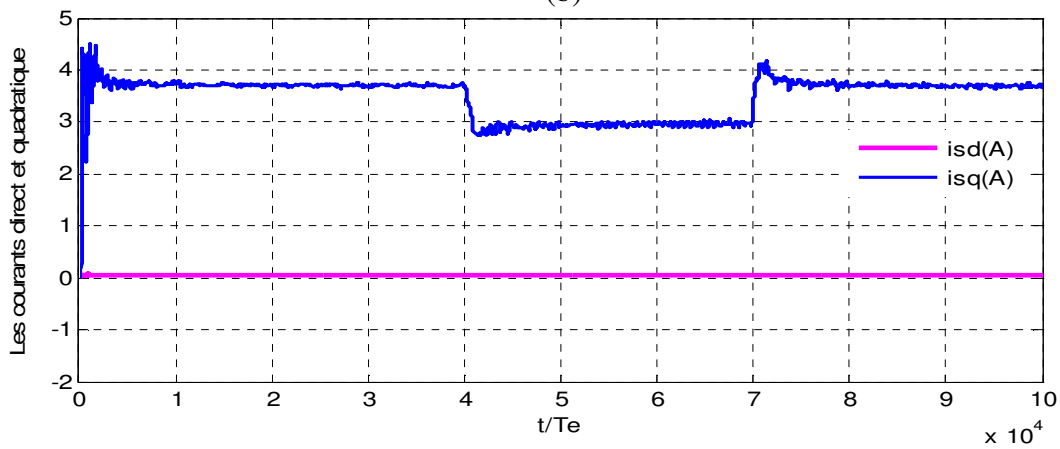

(c)

Figure .2: Performance in pursuit of the trajectory of the controlled system CPNLVM

(a) Speed, (b) Speed Error, (c) Direct and quadratic current

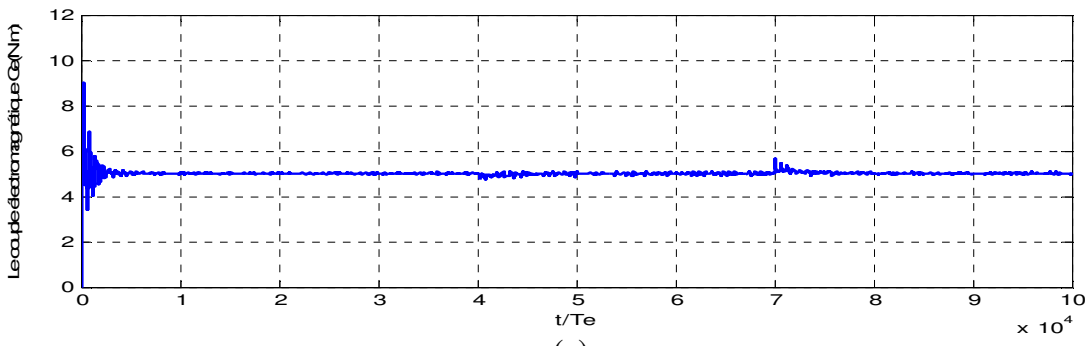

(a)

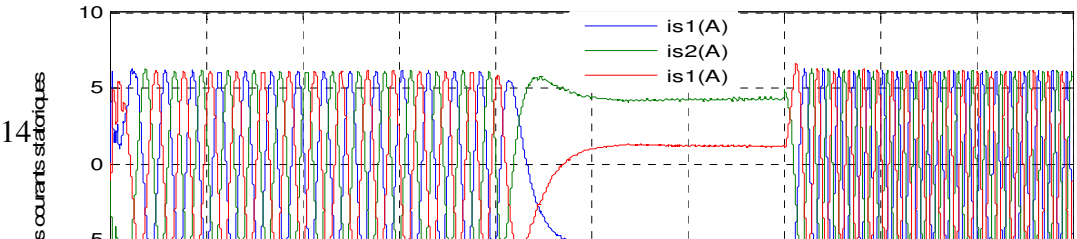

(b)

Figure .3: Performance in pursuit of the trajectory of the controlled system CPNLVM

(a) The Electromagnetic Torque, (b) The stator current of phase 1

4.2. Rejection of load disturbances

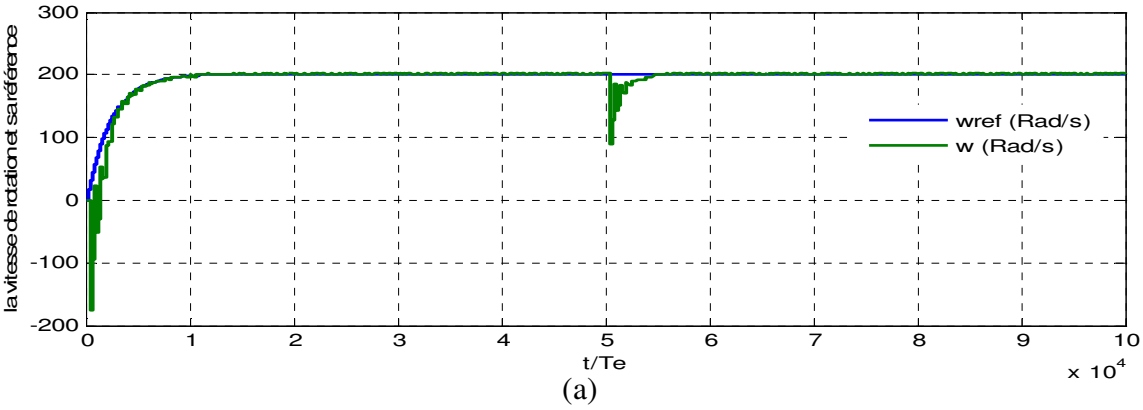

(a)

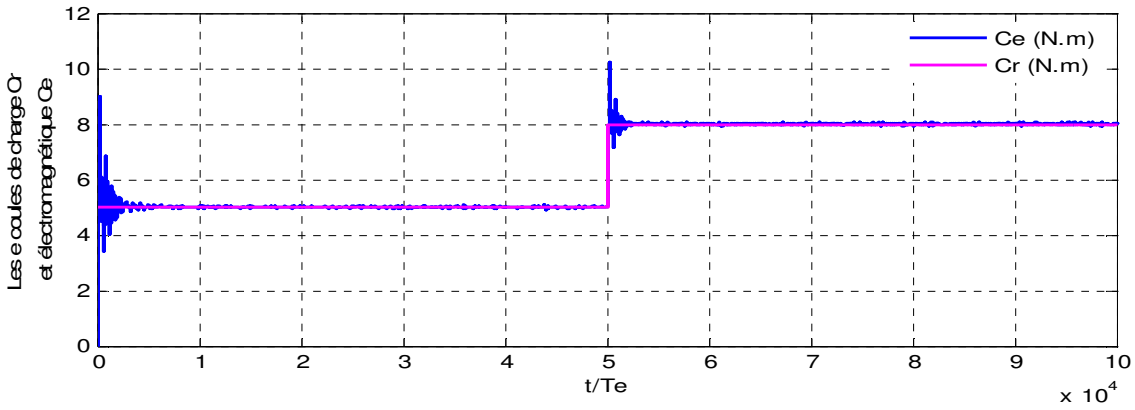

(b)

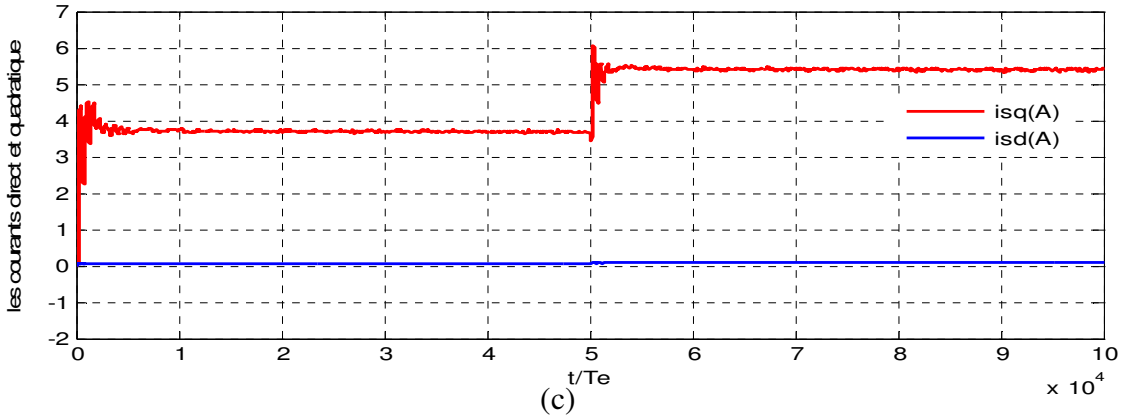

(c)

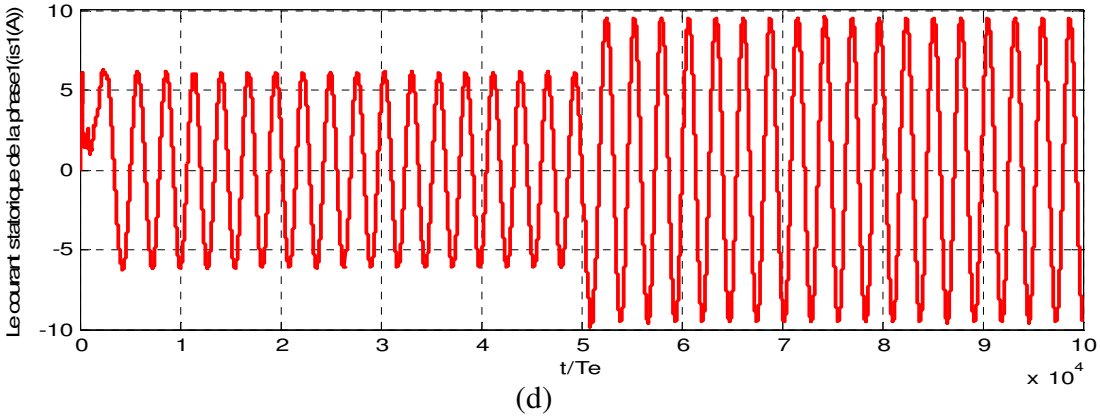

(d)

Figure .4: performance, disturbance rejection, the system with a controller CPNLVM

(a) Speed, (b) Speed error, (c) Direct and quadratic current, (d) The Electromagnetic Torque

4.3. Parametric uncertainties

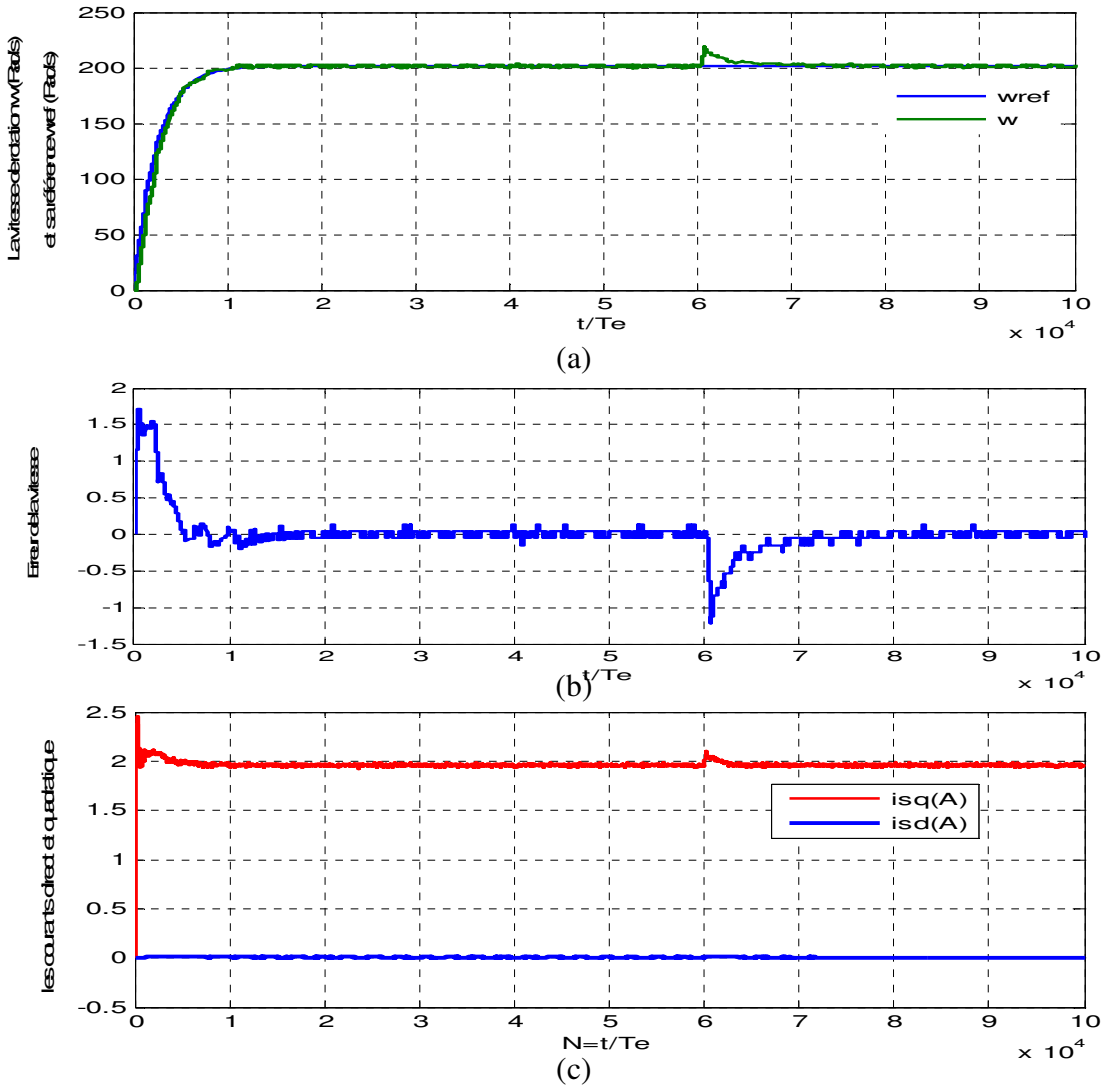

Figure .5: performance driven system CPNLVM in case of variation of the electrical parameters (Rs=0.5Rsn, Lsq=0.5Lsqn, Lsd=0.5Lsdn and Φf=1.2Φfn)) at t=0.3s.

(a) Speed, (b) Speed error, (c) Direct and quadratic current

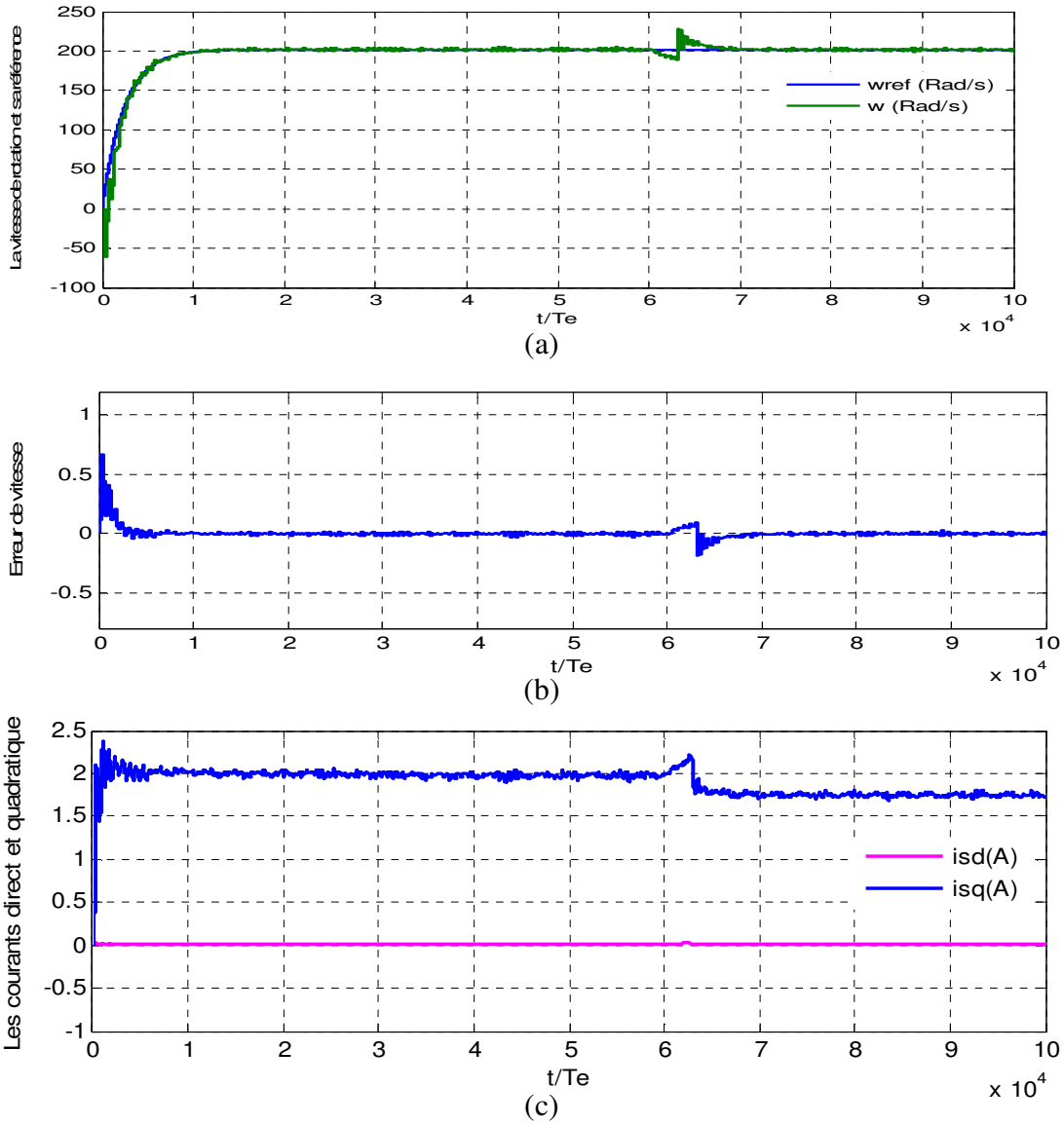

Figure .6: performance driven system CPNLVM in case of variation of mechanical parameters (J=0.5Jn, f=0.5fn) at t=0.3s : (a) Speed, (b) Speed error, (c) Direct and quadratic current

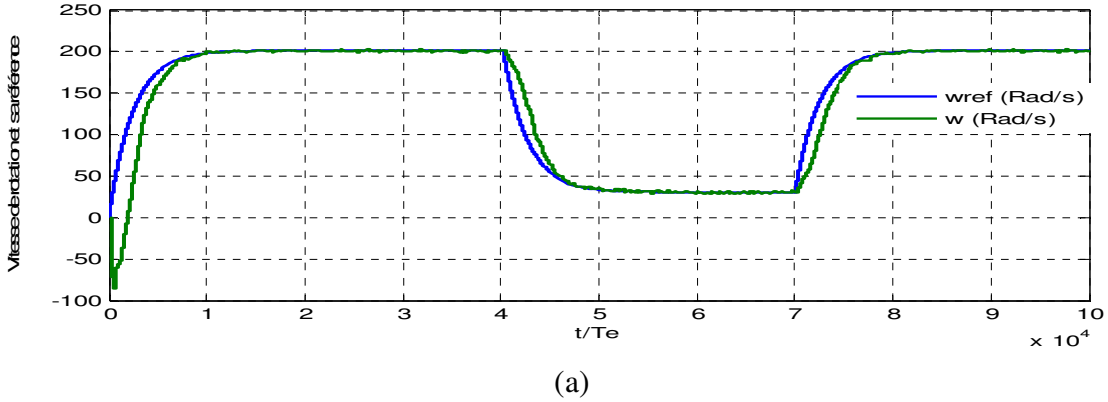

(a)

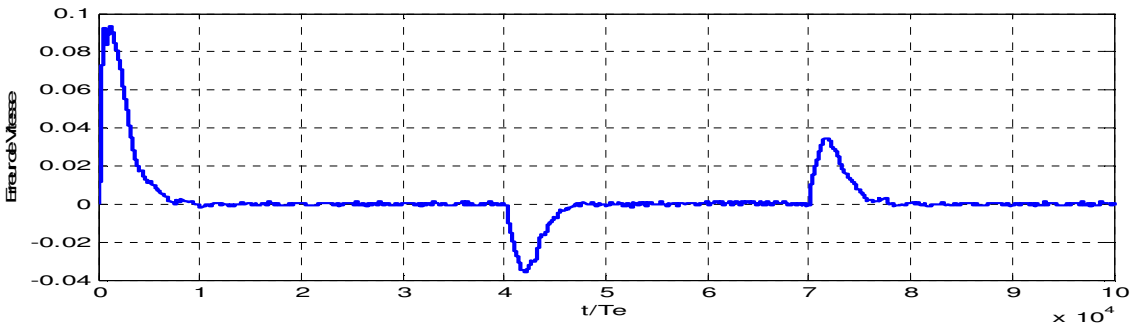

(b)

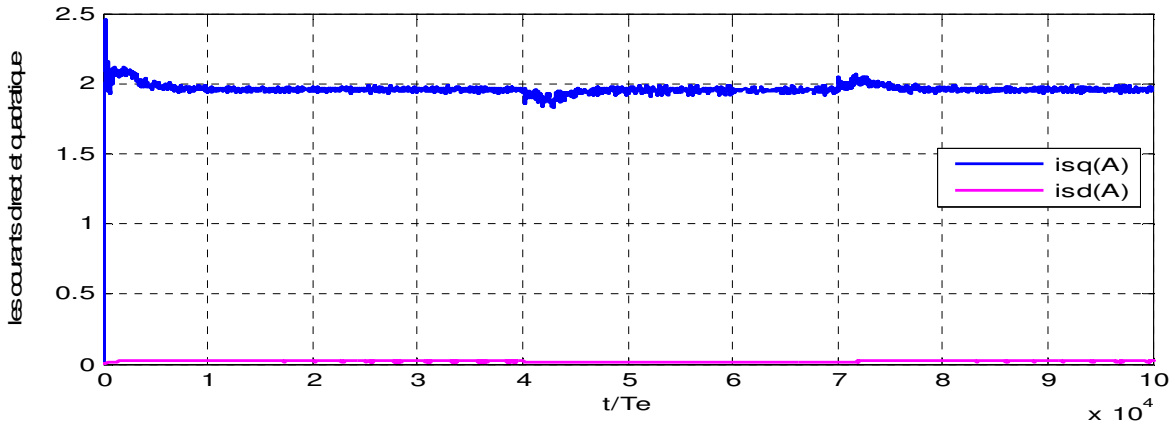

(c)

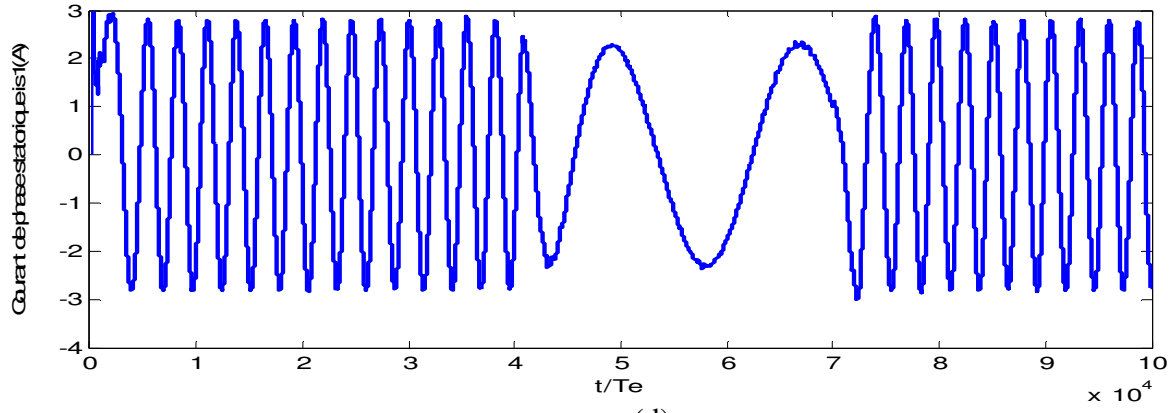

(d)

Figure .7: performance of the controlled system CPNLVM in case of a fast dynamic trajectory without antisaturation scheme

(a) Speed, (b) Speed error, (c) Direct and quadratic current, (d) phase 1 current.

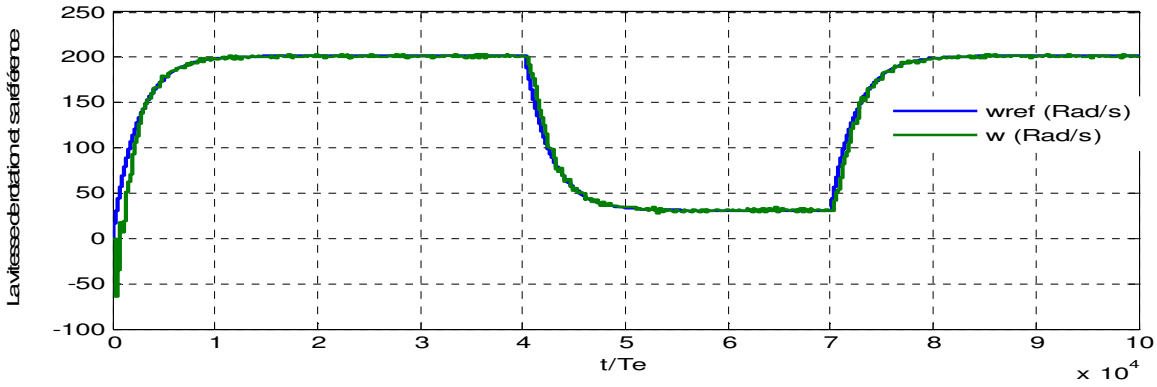

(a)

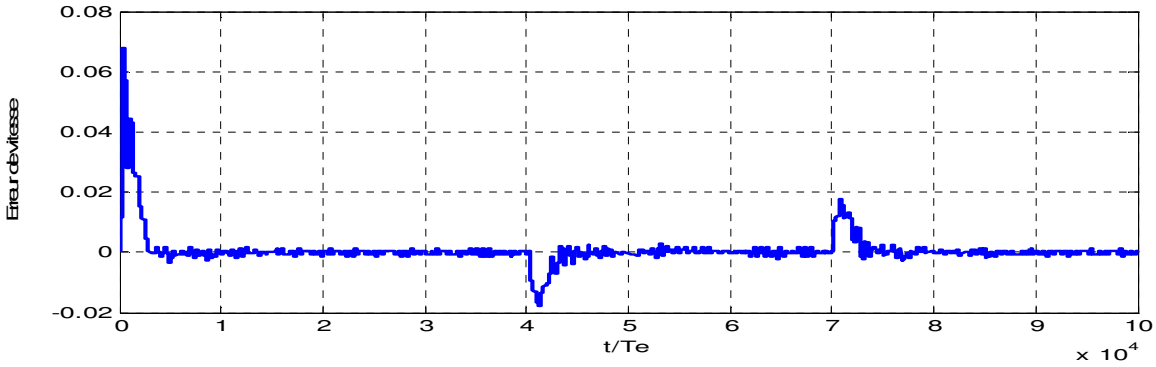

(b)

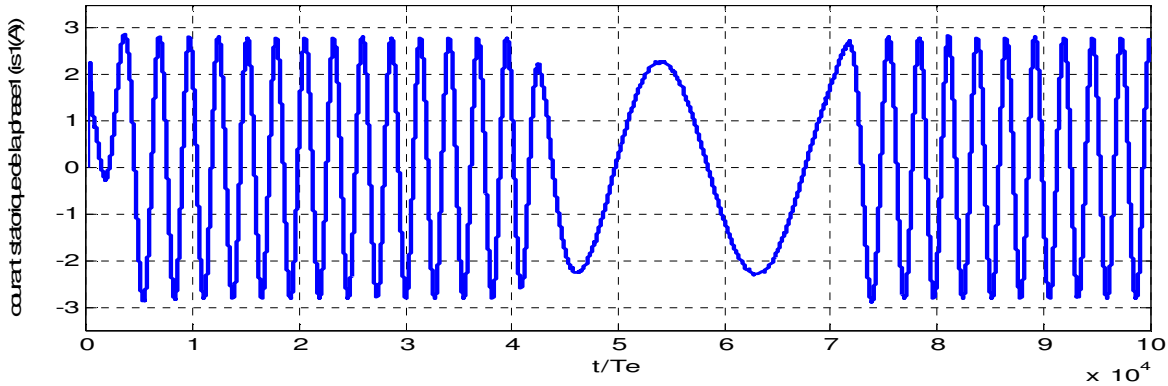

(c)

Figure.8: performance of the controlled system CPNLVM in case of a fast dynamic trajectory with antisaturation scheme: (a) Speed, (b) Speed error, (c) phase 1 current.

From the results obtained, we can see that the introduction of a disturbance observer allowed better tracking path (Figure 2) and the direct current component is kept equal to zero (Figure 2.c).

Regarding the strength vis-à-vis the variation of the electrical and mechanical parameters, Figures 5 and 6 show that the use of compensating in the predictive controller allows the static error of the speed to cancel after a relatively short time, despite the change of all parameters of the machine. On the other hand, with reference to the same figures 5 and 6, we can observe that the direct current component is maintained equal to its reference. Regarding the rejection of disturbance, we can see, from Figure 4 that the predictive controller achieves a perfect speed control. Indeed, at the time of application of the load transient error recorded maximum speed does not exceed 4% and is soon vanish completely.

As for the effectiveness of the anti-saturation diagram, Figure 8 enables us to observe that in the absence of the anti-saturation diagram, the speed in response includes a distance from the path, while the use of the anti-saturation Scheme A have significantly improved dynamic performance by eliminating the excess and reducing the speed of response time (Figure 8a). Note also that the trajectory tracking imposed under the current constraints forces the current to be set to its maximum value (Figures 7 and 8) during transients, which allows for acceleration and deceleration with maximum torque and minimum time. The current fluctuations are due to the modulation of pulse widths.

5. CONCLUSION

In this work, simulation tests were conducted to evaluate the non-linear predictive control on the synchronous machine with permanent magnets. In this context, a non-linear predictive control strategy was proposed and tested, based on the output error.

For this command, we have shown that the use of disturbance observer is required to guarantee vis-à-vis robustness of parametric uncertainties and variation of load torque. The estimators developed from predictive control are based in particular on the integration of the error of the output to regulate, which inevitably led to the elimination of static steady state error.

Regarding the current limitation of the machine, it is assured initially by a path planning and secondly by simple saturation block, and by limiting the manipulated variables from the controller not linear. Taking into account the saturation of blocks in the design of observer's parametric uncertainties and external disturbances has introduced an anti-saturation diagram in the loop of predictive control.

REFERENCES

[1] Bossoufi, B., Karim, M., Lagrioui, A.,(2014) "Matlab & Simulink Simulation with FPGA-Based Implementation adaptative and not adaptative Backstepping nonlinear Control of a Permanent Magnet Synchronous Machine Drive" WSEAS Transactions On Systems And Control, March, Vol.9 No.1, pp 92-103.

[2] Bossoufi, B., Karim, M. Ionita, S., Lagrioui, A., (2011a) "Indirect Sliding Mode Control of a Permanent Magnet Synchronous Machine: FPGA-Based Implementation with Matlab & Simulink Simulation" Journal of Theoretical and Applied Information Technology JATIT, 15 July, Vol. 29 No.1, pp32-42.

[3] Bossoufi, B., Karim, M. Ionita, S., Lagrioui, A. "The Optimal Direct Torque Control of a PMSM drive: FPGA-Based Implementation with Matlab & Simulink Simulation" Journal of Theoretical and Applied Information Technology JATIT, Vol. 28 No.2, pp63-72, 30 June 2011.

[4] Bossoufi, B., Karim, M. Ionita, S., Lagrioui, A "DTC control based artificial neural network for high performance PMSM drive" Journal of Theoretical and Applied Information Technology JATIT, Vol. 33 No.2, pp165-176, 30 November 2011.

[5] Bossoufi, B., Karim, M. Ionita, S., Lagrioui, A. "Nonlinear Non Adaptive Backstepping with Sliding-Mode Torque Control Approach for PMSM Motor" Journal of Journal of Electrical Systems JES, Vol.8 No.2, pp236-248, June 2012.

[6] Bossoufi, B., Karim, M. Ionita, S., Lagrioui, A., EL Hafyani, M.L. "Backstepping control of DFIG Generators for Wide-Range Variable-Speed Wind Turbines " IJAAC International Journal of Automation and Control , pp 122-140, Vol.8 No.2, July 2014.

[7] Bossoufi, B., Karim, M. Ionita, S., Lagrioui, A. "Performance Analysis of Direct Torque Control (DTC) for Synchronous Machine Permanent Magnet (PMSM)" 2010 IEEE 16th International Symposium for Design and Technology of Electronics Packages, IEEE-SIITME'2010, art. No. 5649125, pp. 237-242.Pitesti, Romania.

[8] Bossoufi, B., Karim, M. Ionita, S., Lagrioui, A. "Low-Speed Sensorless Control of PMSM Motor drive Using a Nonlinear Approach Backstepping Control: FPGA-Based Implementation" Journal of Theoretical and Applied Information Technology JATIT, 29 February, Vol. 36 No.1, pp154-166, 29 February 2012.

[9] Melicio, R; Mendes, VMF; Catalao, JPS "Modeling, Control and Simulation of Full- Power Converter Wind Turbines Equipped with Permanent Magnet SynchronousGenerator" vol 5, pg 397-408 Mar - Apr 2010.

[10] J. J. Chen and K. P. Chin, "Automatic flux-weakening control of permanent magnet synchronous motors using a reduced-order controller," IEEE Trans. Power Electron., vol. 15, pp. 881-890, Sept. 2000.

[11] M. Rodic, K. Jezernik, " Speed Sensoless Sliding Mode Torque Control of Induction Motor ", IEEE Trans on. Industrial Electronics, February 2002.

[12] Hisn-Jang Shieh and Kuo-Kai Shyu, "Non Linear Sliding Mode Torque Control With Adaptive Backstepping Approach For Induction Motor Drive", IEEE Transactions on Industrial Electronics, Vol. 46, N° 2, April 1999, pp. 380-388.
[13] D. Zhang and H. Li, "A stochastic-based FPGA controller for an induction motor drive with integrated neural network algorithms," IEEE Trans. Ind. Electron., vol. 55, no. 2, pp. 551–561, Feb. 2008.
[14] C. F. Jung and J. S. Chen, "Water bath temperature control by a recurrent fuzzy controller and its FPGA implementation," IEEE Trans. Ind. Electron., vol. 53, no. 3, pp. 941–949, Jun. 2006.